RESEARCH PAPER

Design and Optimization of Lovastatin-Loaded Fe_3O_4@Mesoporous Silica Nanoparticle-Embedded Oral Fast-Dissolving Films for Enhanced Bioavailability

B. Nandini1, Dr. Y. Dastagiri Reddy. Y[1], Dr. Maheswara Reddy Mallu[2], T. Rajeswari[1], M. Ramachiruhasa Reddy[1] and Dr. D. Maheswara Reddy .D*[1]

[1]*Department of Industrial Pharmacy, Santhiram College of Pharmacy, NH-40, Nandyal- 518501, Andhra Pradesh, India*
[2]*Department of Biotechnology, Koneru Lakshmaiah Education Foundation, Vaddeswaram, Guntur-522302, Andhra Pradesh, India*
[*]***Corresponding author:*** *Dr.D.Maheswara Reddy, Associate Professor, Department of Industrial Pharmacy, Santhiram College of Pharmacy, NH-40, Nandyal, Andhra Pradesh, India*
dagadamahesh@gmail.com

Received: 16th Dec, 2025; Revised: 8th Feb 2026; Accepted: 24th Feb, 2026; Available Online: 30th March, 2026

ABSTRACT

Background: Lovastatin, a Biopharmaceutics Classification System (BCS) Class II drug, exhibits poor aqueous solubility and low oral bioavailability, resulting in limited therapeutic effectiveness. Conventional oral dosage forms suffer from slow dissolution and extensive first-pass metabolism, leading to inadequate drug absorption. Therefore, the development of advanced drug delivery systems such as nanoparticle-based fast-dissolving oral films may improve solubility, dissolution, and bioavailability of lovastatin.

Aim: The present study aimed to design and optimize lovastatin-loaded Fe_3O_4@mesoporous silica nanoparticles incorporated into oral fast-dissolving films to enhance solubility, dissolution rate, and drug permeation.

Methods: Lovastatin-loaded Fe_3O_4@mesoporous silica nanoparticles were prepared and optimized using Box–Behnken Design. The optimized nanoparticles were incorporated into oral fast-dissolving films prepared by solvent casting method. The formulations were characterized for particle size, zeta potential, entrapment efficiency, film thickness, drug content, mechanical strength, and disintegration time. In-vitro dissolution, ex-vivo permeation, and accelerated stability studies were also performed.

Results: The optimized nanoparticles showed particle size of 132 ± 5 nm, polydispersity index of 0.198 ± 0.010, and zeta potential of −28.6 ± 1.4 mV with entrapment efficiency of 88.4 ± 1.8%. The films demonstrated uniform thickness (0.132 ± 0.005 mm), drug content (99.1 ± 1.5%), and rapid disintegration (24 ± 3 s). In-vitro drug release reached 99.1 ± 1.4% within 30 min, while ex-vivo permeation showed 88.7 ± 2.5% drug permeation at 6 h. Stability studies indicated no significant changes over three months.

Conclusion: The developed lovastatin-loaded nanoparticle fast-dissolving films significantly enhanced solubility, dissolution, and permeation, demonstrating potential for improving oral bioavailability.

Keywords: Lovastatin; Fe_3O_4@mesoporous silica; Fast-dissolving film; Nanoparticles; Bioavailability enhancement; Buccal delivery; Box–Behnken design.

How to cite this article: Nandini B, Reddy YD, Mallu MR, Rajeswari T, Reddy MR, Reddy DM, Design and Optimization of Lovastatin-Loaded Fe_3O_4@Mesoporous Silica Nanoparticle-Embedded Oral Fast-Dissolving Films for Enhanced Bioavailability. Int J Drug Deliv Technol. 2026;16(21s): 269-279. DOI: 10.25258/ijddt.16.21s.28

Source of support: Nil.

Conflict of interest: None

1. INTRODUCTION

Hyperlipidemia is a major risk factor for cardiovascular diseases and is characterized by elevated levels of cholesterol, triglycerides, and low-density lipoproteins in the bloodstream. The increasing prevalence of dyslipidemia, particularly in developing countries, has led to a growing demand for effective therapeutic strategies and improved drug delivery systems. Statins remain the first-line therapy for hyperlipidemia, among which lovastatin is widely used due to its ability to inhibit HMG-CoA reductase and reduce cholesterol biosynthesis. However, lovastatin exhibits poor aqueous solubility, low oral bioavailability (<5%), and extensive first-pass metabolism, which significantly limit its therapeutic efficacy and clinical performance. These limitations classify lovastatin as a Biopharmaceutics Classification System (BCS) Class II drug, where dissolution becomes the rate-limiting step for absorption, necessitating the development of advanced delivery approaches. [1-2]

Nanotechnology-based drug delivery systems have emerged as promising strategies to enhance the solubility

**Author for Correspondence: dagadamahesh@gmail.com*

and bioavailability of poorly soluble drugs. Among these, magnetic iron oxide (Fe_3O_4) nanoparticles have gained considerable attention due to their biocompatibility, large surface area, and ease of surface modification. However, bare Fe_3O_4 nanoparticles tend to aggregate and exhibit limited drug loading capacity. To overcome these limitations, coating with mesoporous silica results in Fe_3O_4@mesoporous silica core–shell nanoparticles, which offer improved stability, enhanced drug loading, and controlled drug release. Mesoporous silica nanoparticles possess high surface area, tunable pore size, and excellent physicochemical stability, making them suitable carriers for poorly soluble drugs like lovastatin. [3-5]

In addition to nanocarrier development, the selection of an appropriate dosage form plays a crucial role in improving drug bioavailability. Oral fast-dissolving films (FDFs) have gained significant attention due to their rapid disintegration, ease of administration, and improved patient compliance. These films dissolve quickly in the oral cavity without the need for water and may enhance drug absorption through the buccal mucosa, thereby reducing first-pass metabolism. Incorporation of nanoparticles into fast-dissolving films further enhances drug dissolution, improves permeation, and provides rapid onset of action, making this approach highly suitable for poorly soluble drugs. [6-8]

Therefore, the present study focuses on the design and optimization of lovastatin-loaded Fe_3O_4@mesoporous silica nanoparticles incorporated into oral fast-dissolving films using Box–Behnken Design. This integrated approach aims to enhance drug solubility, dissolution rate, and buccal permeation, thereby improving bioavailability and therapeutic efficacy. The developed system is expected to provide a novel, patient-compliant, and effective drug delivery platform for lovastatin and other poorly soluble drugs.[9,10]

2. MATERIALS AND METHODS

2.1 Materials

Lovastatin was obtained from Yarrow Chem Products, Mumbai, India. Ferric chloride ($FeCl_3$) and ferrous sulfate ($FeSO_4$) were procured from Yarrow Chem Products, Mumbai, India. Ammonia solution was purchased from Rankem Chemicals, India. Cetyltrimethylammonium bromide (CTAB), sodium silicate, polyvinyl alcohol (PVA), and polyethylene glycol 400 (PEG 400) were obtained from SD Fine Chemicals, India. Methanol was purchased from Merck Pvt. Ltd., India. All chemicals used were of analytical grade and used as received.

2.2 Compatibilities studies by FTIR

FTIR studies were carried out to evaluate **drug–excipient compatibility**. The pure drug and physical mixtures of drug with excipients were mixed with potassium bromide (KBr) and compressed into pellets. The samples were scanned in the range of **4000–400 cm^{-1}** using an FTIR spectrophotometer.[11, 12]

2.3 Preparation of Lovastatin-Loaded Fe_3O_4@Mesoporous Silica Nanoparticles

Lovastatin-loaded Fe_3O_4@mesoporous silica nanoparticles were prepared in three sequential steps: (i) synthesis of Fe_3O_4 magnetic nanoparticles, (ii) coating with mesoporous silica, and (iii) drug loading of lovastatin.[13-17]

Synthesis of Fe_3O_4 Magnetic Nanoparticles

Fe_3O_4 nanoparticles were prepared using the co-precipitation method. Ferric chloride ($FeCl_3$) and ferrous sulfate ($FeSO_4$) in a molar ratio of 2:1 were dissolved in distilled water under continuous stirring and heated to 70–80 °C. Ammonia solution (25–30%) was added dropwise until the pH reached 10–11, resulting in the formation of a black precipitate of Fe_3O_4 nanoparticles. The reaction mixture was stirred for 30–60 min to ensure complete formation. The nanoparticles were separated using an external magnetic field, washed repeatedly with distilled water and ethanol, and dried at room temperature to obtain Fe_3O_4 nanoparticles.

Preparation of Fe_3O_4@Mesoporous Silica Nanoparticles

The prepared Fe_3O_4 nanoparticles were dispersed in distilled water using ultrasonication. Cetyltrimethylammonium bromide (CTAB) was added as a template agent, and the pH was adjusted to 9–10 using ammonia solution. Sodium silicate solution was then added dropwise under continuous stirring. The pH was adjusted to neutral using dilute hydrochloric acid to initiate silica deposition. The reaction was continued for 2–3 h to form Fe_3O_4@mesoporous silica nanoparticles. The nanoparticles were separated magnetically, washed with distilled water and ethanol, and dried at room temperature.

Drug Loading of Lovastatin

Lovastatin was dissolved in methanol to prepare a drug solution. Fe_3O_4@mesoporous silica nanoparticles were dispersed in the drug solution and stirred for 12–24 h to facilitate drug adsorption into mesopores. The mixture was sonicated and solvent was evaporated under reduced pressure. Drug-loaded nanoparticles were separated magnetically, washed to remove unbound drug, dried, and stored in a desiccator until further use.

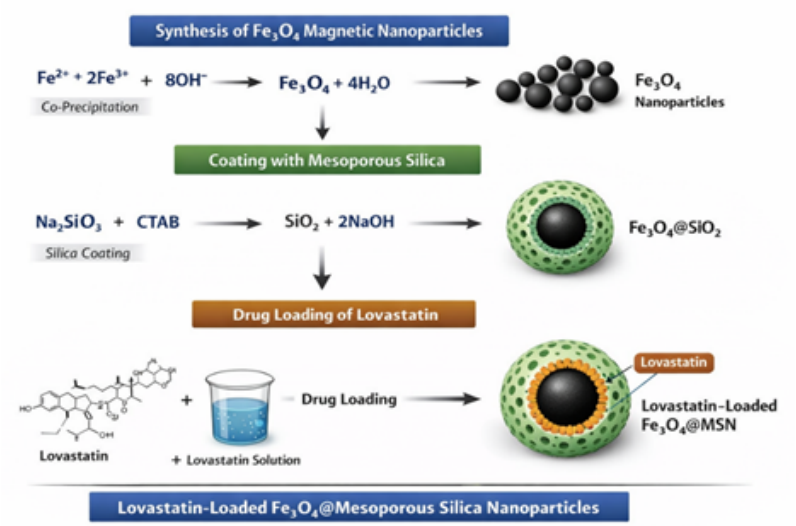

Figure 1: Schematic representation of the preparation of Lovastatin-loaded Fe₃O₄@Mesoporous Silica Nanoparticles via co-precipitation, silica coating, and solvent impregnation method.

Optimization of Lovastatin-Loaded Fe₃O₄@Mesoporous Silica Nanoparticles Using Box–Behnken Design

Box–Behnken Design (BBD) was employed to optimize formulation variables affecting the physicochemical characteristics of lovastatin-loaded Fe₃O₄@mesoporous silica nanoparticles. Based on preliminary screening studies, three independent variables were selected: cetyltrimethylammonium bromide (CTAB) concentration (X_1), sodium silicate volume (X_2), and drug loading time (X_3). Each variable was evaluated at three levels (low, medium, and high) to investigate their effects on nanoparticle properties.[18,19]

The dependent variables selected for optimization included particle size (Y_1) and entrapment efficiency (Y_2), as these parameters play a critical role in determining drug loading capacity and dissolution behavior of nanoparticles. The experimental design matrix was generated using Design-Expert® software (Version 13, Stat-Ease Inc., USA). All formulations were prepared according to the generated design, and the obtained data were analyzed using multiple regression analysis and response surface methodology. The optimized formulation was selected based on desirability function, targeting minimum particle size and maximum entrapment efficiency.

Table 1. Independent Variables and Their Levels in Box–Behnken Design

Factor	Independent Variable	Low (-1)	Medium (0)	High (+1)
X_1	CTAB concentration (%)	0.05	0.525	1
X_2	Sodium silicate (mL)	0.5	0.75	1
X_3	Drug loading time (h)	2	4	6
Factor	**Dependent Variable**	**Goals**		
Y1	Particle size (nm)	Minimize		
Y2	Entrapment efficiency (%)	Maximize		

Smaller particle size (Y_1) was targeted to enhance surface area and improve drug dissolution, while higher entrapment efficiency (Y_2) was desired to maximize drug loading within the mesoporous nanoparticles. The optimized formulation was selected based on statistical significance and desirability criteria.

2.4 Characterization of Nanoparticles

The prepared lovastatin-loaded Fe₃O₄@mesoporous silica nanoparticles were characterized to evaluate their physicochemical properties, stability, and drug loading efficiency.

Particle Size and Polydispersity Index (PDI)

The average particle size and polydispersity index (PDI) of nanoparticles were determined using dynamic light scattering (DLS) technique (Malvern Zetasizer). The nanoparticle suspension was appropriately diluted with distilled water to avoid multiple scattering effects and placed in a cuvette for analysis. Particle size provides information regarding surface area and dissolution behavior, whereas PDI indicates the uniformity of particle size distribution.[20]

Zeta Potential Measurement

Zeta potential of nanoparticles was measured using a zeta potential analyzer based on electrophoretic mobility. The diluted nanoparticle suspension was placed in a specialized cell, and an electric field was applied to determine surface charge. The zeta potential values were used to evaluate the stability of nanoparticle dispersion.[21]

Entrapment Efficiency (EE%)

Entrapment efficiency was determined by centrifugation method. The nanoparticle suspension was centrifuged at high speed to separate free drug from nanoparticles. The

supernatant was collected and analyzed using a UV–Visible spectrophotometer.[22] Entrapment efficiency was calculated using the following formula:

EE(%)=Total drug−Free drug/Total drug×100

Drug Loading Capacity

Drug loading capacity was determined by dissolving nanoparticles in a suitable solvent followed by analysis using UV–Visible spectrophotometry. Drug loading was calculated as the percentage of drug present relative to total nanoparticle weight.

Surface Morphology (SEM Analysis)

The surface morphology of nanoparticles was examined using scanning electron microscopy (SEM). A small quantity of sample was mounted on a sample holder and coated with conductive material. Images were obtained at different magnifications to evaluate shape, size, and surface characteristics of nanoparticles.[23]

Formulation of Fast-Dissolving Oral Films

Fast-dissolving oral films containing lovastatin-loaded Fe_3O_4@mesoporous silica nanoparticles were prepared using the solvent casting method. Accurately weighed polyvinyl alcohol (PVA) (2–4% w/v) was dissolved in distilled water under continuous stirring and heated to 60–70 °C until a clear polymeric solution was obtained. Polyethylene glycol 400 (PEG 400) (0.5–1% w/v) was then added as a plasticizer and mixed thoroughly to improve film flexibility.[24, 25]

The optimized lovastatin-loaded nanoparticles equivalent to the required drug dose were dispersed in a small amount of distilled water and added to the polymeric solution under continuous stirring. The mixture was further stirred for 30–60 minutes and subjected to ultrasonication for 10–15 minutes to remove entrapped air bubbles and ensure uniform dispersion.

The resulting solution was poured onto a leveled glass plate or Petri dish and spread uniformly to obtain films of desired thickness. The films were dried at room temperature for 24 hours or in a hot air oven at 40–45 °C. After drying, the films were carefully peeled off and cut into uniform strips of required size. The prepared films were wrapped in aluminum foil and stored in a desiccator until further evaluation.

Evaluation of Fast-Dissolving Films

The prepared fast-dissolving films were evaluated for physicochemical and mechanical properties. Thickness was measured using a digital micrometer at three different positions, and weight uniformity was determined using a digital analytical balance. Folding endurance was assessed by repeatedly folding the film until it broke, while tensile strength was measured using a texture analyzer.

Surface pH was determined after moistening the film with distilled water to ensure compatibility with oral mucosa. Drug content uniformity was evaluated by dissolving the film in a suitable solvent and analyzing using a UV–Visible spectrophotometer. Disintegration time was determined by placing the film in simulated saliva fluid and recording the time required for complete disintegration.[26]

***In-vitro* Dissolution Study**

In-vitro dissolution studies were carried out using USP Type II (paddle) dissolution apparatus. Phosphate buffer (pH 6.8) was used as dissolution medium to simulate salivary conditions. A fixed volume of 900 mL dissolution medium was maintained at 37 ± 0.5 °C, and paddle rotation speed was set at 50 rpm. The fast-dissolving film equivalent to the required dose was placed in the dissolution medium. Aliquots (5 mL) were withdrawn at predetermined intervals (2, 5, 10, 15, and 30 min) and replaced with fresh medium to maintain constant volume. The samples were filtered and analyzed using a UV–Visible spectrophotometer at the λmax of lovastatin. The cumulative percentage drug release was calculated and plotted against time.[27]

Drug Release Kinetics

The in-vitro drug release data were fitted to various kinetic models including zero-order, first-order, Higuchi, and Korsmeyer–Peppas models to determine the drug release mechanism. The cumulative percentage drug release data were transformed according to each model and plotted. The correlation coefficient (R^2) values were calculated, and the model showing the highest R^2 value was considered as the best-fit model.[28]

***Ex-vivo* Permeation Study**

Fresh goat buccal mucosa was obtained from a local slaughterhouse and transported in cold phosphate buffer. The tissue was cleaned and mounted between donor and receptor compartments of a Franz diffusion cell. The receptor compartment was filled with phosphate buffer (pH 6.8) and maintained at 37 ± 0.5 °C with continuous stirring. The film was placed on the mucosal surface in the donor compartment. Samples were withdrawn at predetermined intervals and replaced with fresh medium. The collected samples were analyzed using UV spectrophotometry, and cumulative drug permeation, flux, and permeability coefficient were calculated.[29]

Stability Studies

Stability studies were conducted according to ICH Q1A(R2) guidelines. Optimized nanoparticle-loaded fast-dissolving films were wrapped in aluminum foil and stored under accelerated conditions (40 ± 2 °C / 75 ± 5% RH) for 3 months. Samples were withdrawn at 0, 1, 2, and 3 months and evaluated for physical appearance, drug content, disintegration time, and in-vitro drug release to assess formulation stability. [30]

3. RESULTS AND DISCUSSION

Fourier Transform Infrared Spectroscopy (FTIR) Study

The FTIR spectrum of pure lovastatin showed characteristic peaks at ~3540 cm^{-1} (O–H stretching), ~2925 cm^{-1} (C–H stretching), ~1725 cm^{-1} (C=O stretching), and ~1260 cm^{-1} (C–O stretching). The drug–

excipient physical mixture retained all important peaks with minor shifts and no new peak formation. These results indicate the absence of chemical interaction between lovastatin and excipients, confirming drug compatibility and stability during formulation.

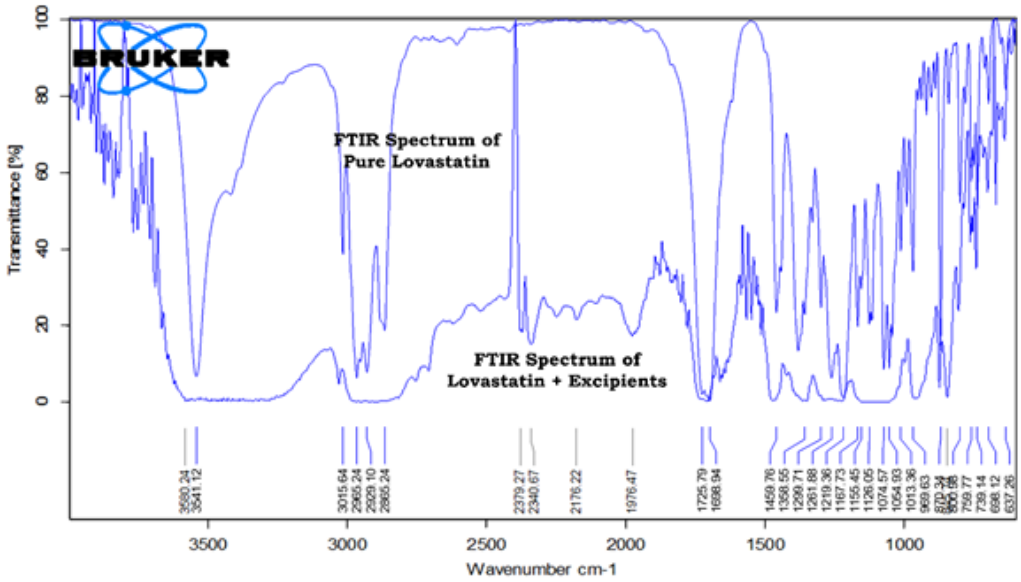

Figure 2. FTIR spectra of pure Lovastatin and Lovastatin–excipient physical mixture showing compatibility.

Optimization Using Box–Behnken Design (BBD)

Box–Behnken Design (BBD) was employed to optimize formulation variables influencing the characteristics of lovastatin-loaded Fe_3O_4@mesoporous silica nanoparticles. Based on preliminary studies, three independent variables were selected: CTAB concentration (A), sodium silicate concentration (B), and drug loading time (C). The dependent responses selected were particle size (Y_1) and entrapment efficiency (Y_2), as these parameters significantly influence nanoparticle performance and drug delivery efficiency. The experimental runs were generated using Design-Expert® software, and the obtained data were analyzed using regression analysis and response surface methodology.

Statistical Analysis and Model Fitting

The statistical analysis of experimental data was performed using ANOVA to evaluate the significance of formulation variables. The model for particle size and entrapment efficiency was found to be statistically significant ($p < 0.0001$), indicating the suitability of the selected model for optimization.

For particle size, CTAB concentration showed the most significant effect, followed by sodium silicate concentration and drug loading time. Increasing CTAB concentration decreased particle size due to improved stabilization and reduced aggregation. In contrast, increasing sodium silicate concentration increased particle size due to thicker silica shell formation. Drug loading time showed a moderate effect on particle size reduction.

Similarly, for entrapment efficiency, CTAB concentration and drug loading time exhibited significant positive effects, whereas sodium silicate concentration showed a minor negative effect. Increased CTAB concentration enhanced nanoparticle stability and surface area, thereby improving drug loading. Longer drug loading time allowed greater drug diffusion into nanopores, resulting in higher entrapment efficiency.

Table 2. ANOVA, Regression Analysis and Polynomial Equations for Particle Size and Entrapment Efficiency

Parameter	Particle Size	Entrapment Efficiency
Model F-value	222.90	248.63
p-value	<0.0001	<0.0001
R^2	0.9926	0.9933
Adjusted R^2	0.9881	0.9893
Predicted R^2	0.9696	0.9691
CV (%)	2.70	1.24
Adequate Precision	50.65	58.21

Polynomial Equation:

Particle Size:

Particle Size = 224.12 − 73.75A + 22.13B − 10.38C − 10.75AB − 5.75AC

Entrapment Efficiency:

EE = 70.03 + 9.89A − 1.07B + 6.31C − 0.625AB + 1.60AC − 0.275BC

The polynomial equations indicate that CTAB concentration has the most significant effect on both responses, while sodium silicate concentration and drug loading time showed moderate influence.

Effect of Formulation Variables on Responses

Effect on Particle Size

Particle size decreased significantly with increasing CTAB concentration due to reduced interfacial tension and improved stabilization of nanoparticles. Sodium silicate concentration showed a positive effect on particle size due to thicker silica coating. Drug loading time slightly reduced particle size due to improved dispersion and stabilization.

Effect on Entrapment Efficiency

Entrapment efficiency increased with increasing CTAB concentration and drug loading time. Higher CTAB concentration improved nanoparticle stability and increased drug adsorption. Longer loading time allowed drug diffusion into mesopores, enhancing entrapment efficiency. Sodium silicate showed a slight negative effect due to dense silica structure formation.

Response Surface Analysis

The contour and 3D surface plots were used to visualize the influence of formulation variables on particle size and entrapment efficiency. The plots showed that higher CTAB concentration and moderate sodium silicate levels resulted in minimum particle size and maximum entrapment efficiency.

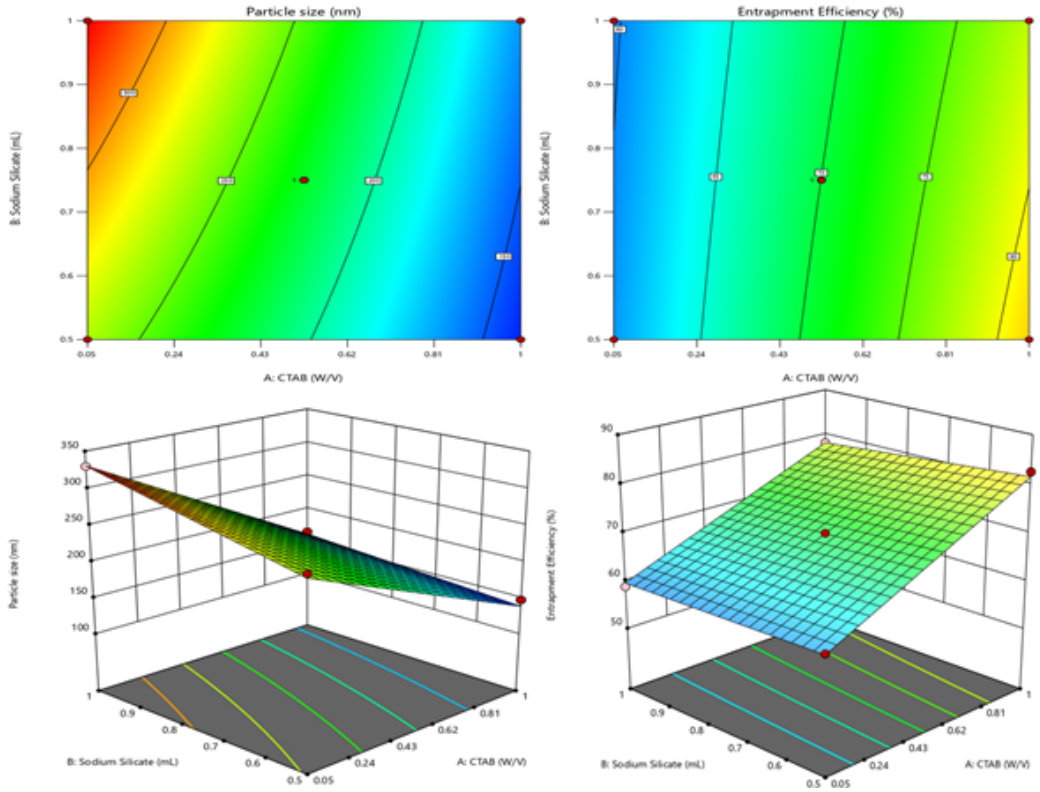

Figure 3. Contour and 3D Surface Plots Showing Effect of Formulation Variables on Particle Size and Entrapment Efficiency

The response surface analysis confirmed that CTAB concentration was the most influential factor affecting both responses. The optimum region was observed at higher CTAB concentration and moderate sodium silicate levels.

Optimization Using Desirability Function

The optimization was performed using desirability function approach to obtain minimum particle size and maximum entrapment efficiency. The optimized formulation showed high desirability value indicating ideal formulation conditions.

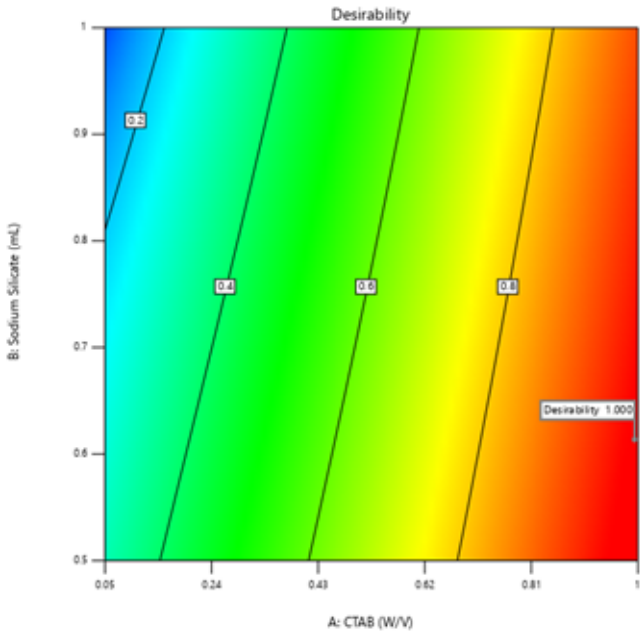

Figure 4. Desirability Plot for Optimization of Lovastatin-Loaded Fe_3O_4@MSN Nanoparticles

Validation of Optimized Formulation

The optimized formulation was prepared and evaluated to validate the model. The observed values were found to be in close agreement with predicted values, indicating the reliability of the optimization model.

Table 3. Predicted and Observed Values of Optimized Formulation

Parameter	Predicted Value	Observed Value (Mean ± SD)
Particle Size (nm)	129.63	131.06 ± 2.51
Entrapment Efficiency (%)	88.47	87.83 ± 1.70

The minimal deviation between predicted and observed values confirms the accuracy and robustness of the optimization model. The optimized formulation was selected for further incorporation into fast-dissolving films.

Polydispersity Index (PDI) Analysis

Polydispersity index (PDI) was evaluated to determine the uniformity of nanoparticle size distribution. The PDI values ranged from **0.198 to 0.462**, indicating variation among formulations. Lower PDI values (<0.3) indicate uniform particle distribution, whereas higher values (>0.4) suggest heterogeneity.

The optimized formulation (Run 5) showed the lowest PDI (**0.198 ± 0.010**), indicating a narrow size distribution and uniform nanoparticle population. Formulations with larger particle sizes exhibited higher PDI values, likely due to aggregation and non-uniform particle growth.

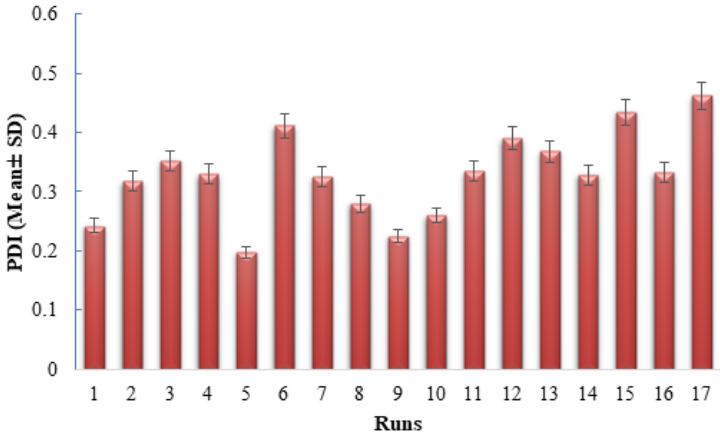

Figure 5. Polydispersity Index of Lovastatin-Loaded Fe_3O_4@SiO_2 Nanoparticles

Zeta Potential Analysis

The zeta potential of the optimized formulation was found to be **−28.6 ± 1.4 mV**, indicating good electrostatic stability of nanoparticles. The negative surface charge may be attributed to the presence of silica and surface functional groups.

A zeta potential value greater than ±25 mV suggests stable nanoparticle dispersion due to electrostatic repulsion, which prevents aggregation. Therefore, the optimized formulation was considered physically stable.

Scanning Electron Microscopy (SEM) Analysis

Scanning electron microscopy (SEM) was performed to evaluate the surface morphology of the optimized nanoparticles. The SEM images revealed spherical nanoparticles with smooth surface morphology and uniform distribution. Minimal aggregation was observed, which correlates with the low PDI value of the optimized formulation.

The particle size observed in SEM images was consistent with dynamic light scattering results (~130 nm). The smooth surface morphology confirms successful silica coating over the Fe_3O_4 core, indicating formation of core–shell nanoparticles with good structural integrity.

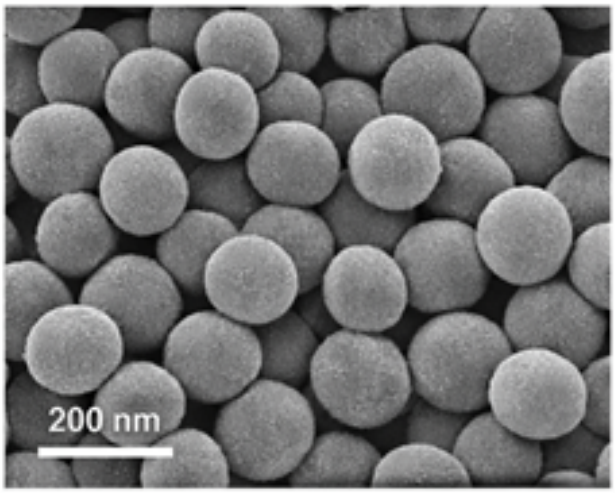

Figure 6. SEM images of optimized Lovastatin-loaded Fe_3O_4@SiO_2 nanoparticles showing spherical morphology and uniform distribution.

Evaluation of Fast-Dissolving Films

The fast-dissolving oral films containing lovastatin-loaded Fe_3O_4@SiO_2 nanoparticles were evaluated for physicochemical and mechanical properties. The results demonstrated that both conventional film (CF) and nanoparticle-loaded film (NF) exhibited acceptable characteristics suitable for oral drug delivery.

The thickness and weight variation of films were uniform, indicating reproducible film casting. The slight increase observed in NF may be attributed to the incorporation of nanoparticles into the polymer matrix. Folding endurance values above 150 folds confirmed good flexibility and mechanical strength of the films. Surface pH values were close to neutral, suggesting compatibility with oral mucosa and reduced risk of irritation.

The nanoparticle-loaded film showed improved drug content uniformity (99.1 ± 1.5%) compared to conventional film, indicating uniform dispersion of nanoparticles. A significant reduction in disintegration time was observed in NF (24 ± 3 sec) compared to CF (38 ± 4 sec), suggesting rapid film dissolution due to the porous nature of nanoparticles. Additionally, NF exhibited slightly higher tensile strength, indicating enhanced mechanical integrity. Overall, nanoparticle-loaded films demonstrated improved drug distribution, faster disintegration, and acceptable mechanical properties, indicating their suitability for rapid oral drug delivery.

Table 4. Evaluation Parameters of Conventional Film (CF) and Nanoparticle-Loaded Film (NF)

Parameter	CF (Conventional Film)	NF (NP-Loaded Film)
Thickness (mm)	0.128 ± 0.004	0.132 ± 0.005
Weight variation (mg)	52.4 ± 1.8	54.1 ± 2.0
Folding endurance (no. of folds)	172 ± 8	165 ± 7
Surface pH	6.7 ± 0.2	6.8 ± 0.1
Drug content uniformity (%)	97.3 ± 1.9	99.1 ± 1.5
Disintegration time (sec)	38 ± 4	24 ± 3
Tensile strength (N/mm²)	2.31 ± 0.18	2.45 ± 0.20

In-vitro Dissolution Studies

The *in-vitro* dissolution studies were carried out using USP Apparatus II (paddle method) in phosphate buffer (pH 6.8) maintained at **37 ± 0.5 °C** and 50 rpm. The dissolution profiles of pure lovastatin, conventional film (CF), and nanoparticle-loaded film (NF) were compared to evaluate the effect of nanoparticle incorporation on drug release.

Pure lovastatin showed slow and incomplete drug release, with only **48.6 ± 3.2%** release at 30 minutes, which may be attributed to poor aqueous solubility and crystalline nature of the drug. In contrast, the conventional film showed improved drug release (**90.8 ± 2.3% at 30 min**) due to rapid film disintegration and increased surface area.

The nanoparticle-loaded film exhibited significantly enhanced drug release, achieving **94.2 ± 2.1% within 15 minutes** and **99.1 ± 1.4% at 30 minutes**. The improved dissolution behavior may be attributed to reduced particle size, mesoporous silica structure, improved wettability, and rapid film disintegration.

Comparative analysis demonstrated enhanced dissolution in the order: **NF > CF > Pure Drug**, confirming the effectiveness of nanoparticle incorporation in improving drug release and dissolution rate.

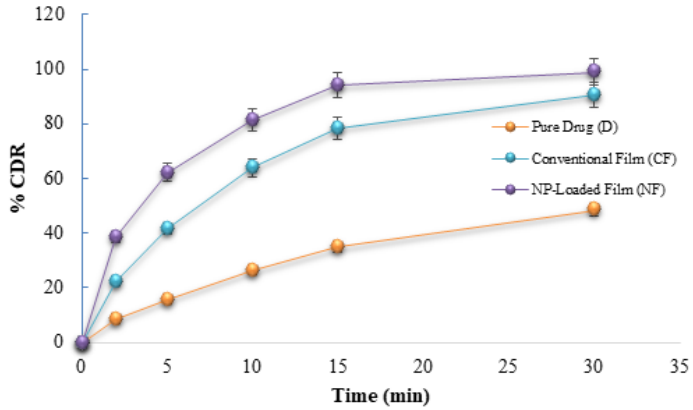

Figure 7. Comparative in-vitro drug release profiles of pure lovastatin, conventional film, and nanoparticle-loaded fast-dissolving film

Drug Release Kinetics of NP-Loaded Fast-Dissolving Film

The in-vitro drug release data of the nanoparticle-loaded fast-dissolving film (NF) were fitted to various kinetic models including zero-order, first-order, Higuchi, and Korsmeyer–Peppas models to determine the drug release mechanism.

The Higuchi model showed the highest correlation coefficient (R^2 = 0.989), indicating that drug release predominantly follows a diffusion-controlled mechanism. The Korsmeyer–Peppas model also showed good correlation (R^2 = 0.982) with a release exponent (n = 0.68), indicating non-Fickian diffusion. This suggests that drug release is governed by a combination of diffusion and polymer relaxation.

Overall, the results indicate that lovastatin release from nanoparticle-loaded films occurs through diffusion from mesoporous nanoparticles along with rapid film disintegration, resulting in enhanced dissolution and improved drug availability.

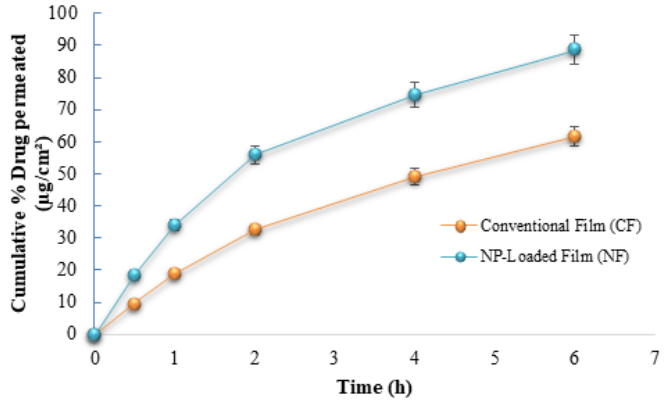

Figure 8. Comparative ex-vivo drug permeation profiles of conventional film and nanoparticle-loaded fast-dissolving film across goat buccal mucosa

Stability Studies

Stability studies of the optimized nanoparticle-loaded fast-dissolving film were conducted under accelerated conditions (40 ± 2 °C / 75 ± 5% RH) for 3 months. No significant change in physical appearance was observed during the study period.

The drug content showed a slight decrease from **99.1 ± 1.5% to 97.8 ± 1.9%**, remaining within acceptable limits. Disintegration time slightly increased from **24 ± 3 sec to 27 ± 4 sec**, while drug release at 15 minutes showed a minor reduction from **94.2 ± 2.1% to 91.9 ± 2.7%**.

These results indicate that the formulation remained stable with minimal variation in physicochemical properties and drug release behavior, confirming its suitability for storage.

CONCLUSION

The present study successfully developed and evaluated **lovastatin-loaded Fe_3O_4@SiO_2 nanoparticle incorporated fast-dissolving films** to enhance solubility, dissolution, and permeation of lovastatin. The drug exhibited poor aqueous solubility (**0.42 ± 0.05 µg/mL**) and a high partition coefficient (**log P = 3.62 ± 0.12**), justifying the need for formulation development. The optimized nanoparticles showed a **particle size of 132 ± 5 nm, entrapment efficiency of 88.4 ± 1.8%, PDI of 0.198 ± 0.010**, and **zeta potential of −28.6 ± 1.4 mV**, indicating uniformity and stability.

The incorporation of nanoparticles into fast-dissolving films resulted in desirable physicochemical and mechanical properties, including **uniform thickness (0.132 ± 0.005 mm), high drug content (99.1 ± 1.5%)**, and **rapid disintegration time (24 ± 3 sec)**. The nanoparticle-loaded film demonstrated significantly enhanced drug release, achieving **99.1 ± 1.4% release within 30 minutes**, compared to pure drug (**48.6%**) and conventional film (**90.8%**).

Ex-vivo permeation studies further confirmed improved drug delivery, with **88.7 ± 2.5% permeation at 6 hours, flux of 78.6 ± 4.2 µg/cm²/h**, and **permeability coefficient of 3.6×10^{-3} cm/h**, which were significantly higher than the conventional formulation. Stability studies indicated no significant changes over 3 months, with drug content maintained at **97.8%** and drug release at **91.9%**.

Overall, the developed formulation demonstrated **rapid release, enhanced permeation, and good stability**, making it a promising approach for improving the oral bioavailability of lovastatin.

4. ACKNOWLEDGMENT

The authors express their sincere gratitude to **Santhiram College of Pharmacy, Nandyal**, for providing necessary facilities and support to carry out this research work. The authors also thank the laboratory staff for their technical assistance.

5. CONFLICT OF INTEREST

The authors declare that there is no conflict of interest regarding the publication of this manuscript.

6. FUNDING STATEMENT

This research received **no specific grant** from any funding agency in the public, commercial, or not-for-profit sectors.

7. AUTHOR CONTRIBUTIONS

All authors contributed to the conceptualization, methodology, investigation, data analysis, and manuscript preparation. All authors reviewed and approved the final version of the manuscript. The corresponding author supervised the overall research work.

8. DATA AVAILABILITY STATEMENT

The data supporting the findings of this study are available from the corresponding author upon reasonable request.

9. ETHICAL APPROVAL

No human or animal studies were performed in this research. The *ex-vivo* study using goat buccal mucosa was conducted in accordance with institutional guidelines.

10. REFERENCES

1. Libby P. Inflammation in atherosclerosis. *Nature*. 2002;420(6917):868–874.
2. Nelson RH. Hyperlipidemia as a risk factor for cardiovascular disease. *Primary Care*. 2013;40(1):195-211.
3. Istvan ES, Deisenhofer J. Structural mechanism for statin inhibition of HMG-CoA reductase. *Science*. 2001;292(5519):1160-1164.
4. Lennernäs H, Fager G. Pharmacodynamics and pharmacokinetics of lovastatin. *Clin Pharmacokinet*. 1997;32(5):403-425.
5. Amidon GL, Lennernas H, Shah VP, Crison JR. A theoretical basis for a Biopharmaceutics Drug Classification. *Pharm Res*. 1995;12(3):413-420.
6. Lipinski CA. Poor solubility challenges in drug discovery. *Adv Drug Deliv Rev*. 2001;46(1-3):3-26.
7. Patel A, Cholkar K, Agrahari V, Mitra AK. Nanotechnology-based approaches for enhanced bioavailability. *AAPS PharmSciTech*. 2012;13(2): 426-435.
8. Laurent S, Forge D, Port M, Roch A, Robic C, Vander Elst L, Muller RN. Magnetic iron oxide nanoparticles: synthesis and biomedical applications. *Chem Rev*. 2008;108(6):2064-2110.
9. Lu AH, Salabas EL, Schüth F. Magnetic nanoparticles: synthesis, protection, functionalization. *Angew Chem Int Ed*. 2007;46(8):1222-1244.
10. Slowing II, Trewyn BG, Lin VS. Mesoporous silica nanoparticles for drug delivery. *J Am Chem Soc*. 2006;128(46):14792-14793.

11. Stuart B. Infrared Spectroscopy: Fundamentals and Applications. Wiley; 2004.
12. Silverstein RM, Webster FX, Kiemle DJ. Spectrometric Identification of Organic Compounds. Wiley; 2005.
13. Massart R. Preparation of aqueous magnetic liquids. *IEEE Trans Magn*. 1981;17(2):1247-1248.
14. Laurent S, Forge D, Port M, et al. Magnetic iron oxide nanoparticles: synthesis and biomedical applications. *Chem Rev*. 2008;108:2064-2110.
15. Slowing II, Trewyn BG, Lin VSY. Mesoporous silica nanoparticles for drug delivery. *J Am Chem Soc*. 2006;128:14792-14793.
16. Vallet-Regí M, Balas F, Arcos D. Mesoporous materials for drug delivery. *Angew Chem Int Ed*. 2007;46:7548-7558.
17. Trewyn BG, Slowing II, Giri S, et al. Synthesis and functionalization of mesoporous silica nanoparticles. *Acc Chem Res*. 2007;40:846-853.
18. Ferreira SL, Bruns RE, Ferreira HS, et al. Box-Behnken design: optimization techniques. *Anal Chim Acta*. 2007;597:179-186.
19. Montgomery DC. Design and Analysis of Experiments. Wiley; 2013.
20. Malvern Instruments. Dynamic Light Scattering Theory Manual. 2011.
21. Hunter RJ. Zeta Potential in Colloid Science. Academic Press; 1981.
22. Mohanraj VJ, Chen Y. Nanoparticles – a review. *Trop J Pharm Res*. 2006;5:561-573.
23. Goldstein JI, et al. Scanning Electron Microscopy and X-Ray Microanalysis. Springer; 2003.
24. Dixit RP, Puthli SP. Oral strip technology. *J Control Release*. 2009;139:94-107.
25. Bala R, Pawar P, Khanna S. Orally dissolving films. *Int J Pharm Investig*. 2013;3:67-76.
26. Boateng JS, Matthews KH, Stevens HN, et al. Buccal drug delivery systems. *J Pharm Sci*. 2008;97:2892-2923.
27. United States Pharmacopeia (USP 43-NF 38). Dissolution Testing. USP Convention; 2020.
28. Korsmeyer RW, Peppas NA. Drug release kinetics. *Int J Pharm*. 1983;15:25-35.
29. Franz TJ. Percutaneous absorption studies. *J Invest Dermatol*. 1975;64:190-195.
30. ICH Q1A(R2). Stability Testing of New Drug Substances and Products. ICH Guidelines; 2003.